IOP Conf. Series: Materials Science and Engineering **398** (2018) 012030 doi:10.1088/1757-899X/398/1/012030

A Dynamic Relation Model Analysis of High-speed Impact and Sabot Strength

H Y Wu, L ZH Wang Y Q Li and M Zhao

School of Mechanical Engineering, Xi'an Jiaotong University,Xi'an,710049,China

E-mail: wuhy@xjtu.edu.cn

Abstract. To understand how a projectile penetrates a sabot during a high-speed impact testing，which led to the failure of the impacting experiment, a dynamic model was built based on the interactions between the projectile and the sabot; and the bearing strengths of the sabot with varying impact speeds were analyzed. The correctness of the model was verified by an experiment. It shows that, with all the other conditions kept the same, the maximum stress between the sabot and the projectile increases with the decrease of the sabot mass, the increase of the projectile and impact speed.

1. **Introduction**

In earlier days, high-speed impact problems mainly appear in the military field, and now they emerges in civilian areas [1]. Air gun is a useful experiment tool for high-speed launching and high pressure loading. It is commonly used for the study of mechanics of materials, penetration, and high-speed impact[2]. The launching tube of the gun normally has a large diameter to meet the broader size experiment requirements. In this condition, a small-size projectile should be supported by a sabot, which traps the propellant gas and keeps the projectile centered in the launching tube while steadily moving forward. The sabot is not an indispensable component, the mass of the sabot is required to be designed as low as possible[3]. When firing, the high pressure gas forces the sabot to carry the projectile down the lauching tube, the contact surface of the sabot suffers huge stress. The material of the sabot should have high strength and good toughness to ensure its structure integrity[4].

Earlier sabots were made of metallic materials, such as red copper, copper alloy, pure iron, aluminum, aluminium alloy, etc. A large number of new materials who are light weight yet have high mechanical strength and good toughness have been appeared, such as various resin materials, fiber glass, carbon fiber, etc. [5]. The majority of the research on the sabot has been focused on the sabot separation process[6,7,8], the structural analysis of the composite sabot[9,10], the motion analysis during sabot opening process[11], sabot opening lift force[12], etc. While this paper focuses on how to keep the projectile and sabot always be a whole to ensure the high impact experiment doing successfully. Polyurethane foam is a good candidate for normal impact experiment which can fulfill the loading requirements with low cost. The strength of polyurethane foam depends on the foaming compactness. If the strength is insufficient, the projectile may penetrate it and causes the experiment failure. The relationships among the required strength of the sabot, the projectile mass and the experimental velocity should be analyzed and built to ensure a successful impact test.

2. The phenomenon of sabot penetrates projectile

The first-class air gun is commonly used during an impact testing. The diameter of the sabot is approximately equal to the diameter of the launching tube, so that it can carry various projectiles with different sizes (Fig. 1).

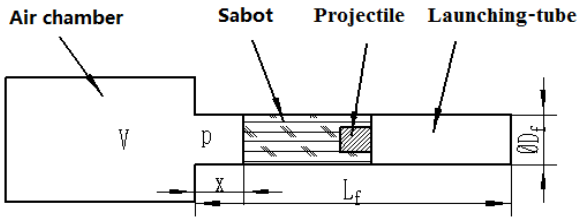

Figure 1. Sketch of projectile and sabot in air gun

When firing, the sabot and the projectile are accelerated instantly by the compressed air, a significant pressure is applied to their contact area. Fig. 2 shows a home-made sabot with density of 47kg/m^3. When the velocity was higher than 145m/s, the projectile penetrated its support sabot and caused the failure of the high speed impact experiment(Fig. 3).

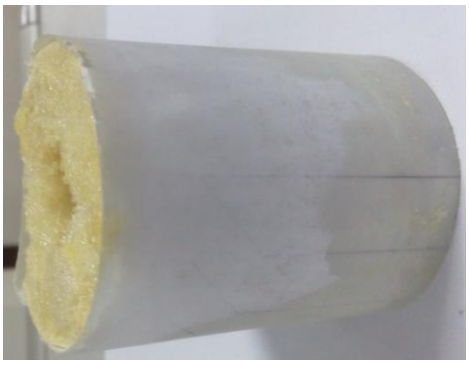

Figure 2. Self-made foam sabot

Fig. 3 showed the moment of the projectile penetrated through the sabot, which was captured by a high speed camera. After recording the sabot at t_1, the projectile rolled into the shot range at t_2. In this condition, there was no way for projectile to hit the target plate with scheduled trajectory and speed. It hit the sabot separator and was rebounded. This led to a complete failure of the experiment. The free flying projectile would easily hit on the sabot separator, and both of them were damaged (Fig. 4), the projectile may not pass through the sabot separator successfully. And the irregular bouncing of projectile may cause severe safety issues. This penetration problem must be solved to ensure the high speed impact examination can be carried out normally.

(a) Sabot at t_1 moment (b) Rolling flying projectile at t_2 moment

Figure 1. High speed camera recording projectile penetrating sabot

Figure 2. Impact damage on the sabot separator and the projectile

It is necessary to find out the relationship between the shear strength of the sabot, the projectile velocity and their mass to ensure a successful high speed impact experiment.

3. Dynamic analysis of interaction force between sabot and projectile

Define m_1 and m_2 as the mass of the sabot and the projectile respectively, ρ_1 and ρ_2 as the density of the them, D_f, S_f and L_f as the diameter, sectional area and effective length of the launching tube, p as the gas pressure at some moment, x as the distance between the projectile and its initial position.
Sabot velocity v is an important parameter in air gun test. It can be estimated by the following formulas. When the gas pushes the projectile, the gas expansion process can be regarded as the ideal gas adiabatic expansion process[13].

$$pV = \frac{M}{\mu_g}RT$$
$$p_{cs}V_{cq}^{\gamma} = p(V_{cq} + S_f x)^{\gamma} \tag{1}$$

In the formula: p—gas pressure; V—space volume behind projectile; μ_g-- the mocular number of gas; M—injected gas mass; R—gas constant; T—gas temperature; γ--gas adiabatic index; S_f -- cross section area of launching tube, $\pi D_f^2/4$; p_{cs}--gas injection pressure of gas chamber; V_{cq}-- initial chamber volume; p_{21}—pressure exerted on sabot by projectile; S_{dw}-- the cross sectional area of the projectile.
The stress analysis of the sabot is carried out when the high pressure air is suddenly released(Fig. 5). The sabot is subjected to the force exerted by compressed air(F_{01})and projectile(F_{21}).

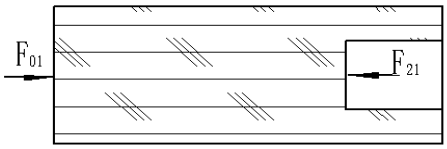

Figure 5. Force analysis of sabot

Without considering the specific forms of various energy loss, the mass of the sabot is increased from m_1 to φm_2 in order to replace various loss factors. So the motion equation of the sabot is as follows:

$$\varphi m_1 \frac{dv}{dt} = F_{01} - F_{21} = pS_f - p_{21}S_{dw} \tag{2}$$

where φ is called virtual mass coefficient, which is calculated as follows in the interior ballistics theory:

$$\varphi = K + \frac{1}{3}\frac{M}{m} \tag{3}$$

The factor K is determined by experiment, which is about 1~1.10. The letter m represents the sum mass of sabot and projectile and M is the mass of the gas.

$$M = \frac{p_{cs}V_{cq}}{RT}\mu_g \tag{4}$$

Eq.(5) is got by calculating Eq.(1) and Eq.(2).

$$\frac{dv}{dt} = \frac{1}{m_1\varphi}\left(\frac{S_f p_{cs}V_{cq}^{\gamma}}{(V_{cq}+S_f x)^{\gamma}} - p_{21}S_{dw}\right) \tag{5}$$

After formula transformation, Eq.(6) can be obtained.

$$vdv = \frac{1}{m_1\varphi}\left(\frac{S_f p_{cs}V_{cq}^{\gamma}}{(V_{cq}+S_f x)^{\gamma}} - p_{21}S_{dw}\right)dx \tag{6}$$

According to the motion consistency, the sabot and projectile can be regarded as one part, the change law of stresses exerted on them are similar to the chamber pressure in launching tube[14], which increases sharply at first then decreases gently (Fig.6). In order to simplify the calculation, it is assumed that the contact stress at the bottom of the projectile increases linearly during the launching process, and k is the linear slope. It is assumed that v_m is the maximum speed and L_m is the moving distance of sabot when the stress between sabot and projectile reaches the peak value. The relation law between p_{21} and x can be expressed as Eq.(7).

$$p_{21}(x) = kx, \quad x \le L_m \tag{7}$$

Eq.(7) is put into Eq.(6), and Eq.(8) is obtained through integral.

$$\int_0^{v_m} vdv = \frac{S_f p_{cs}V_{cq}^{\gamma}}{m_1\varphi}\int_0^{L_m}\frac{dx}{(V_{cq}+S_f x)^{\gamma}}dx - \frac{1}{m_1\varphi}\int_0^{L_m} kxS_{dw}dx, \quad x \le L_m \; v_m^2 = \frac{2p_{cs}V_{cq}}{m_1\varphi(\gamma-1)}\left[1-\frac{V_{cq}^{\gamma-1}}{(V_{cq}+S_f L_m)^{\gamma-1}}\right] - \frac{kS_{dw}L_m^2}{2m_1\varphi} \tag{8}$$

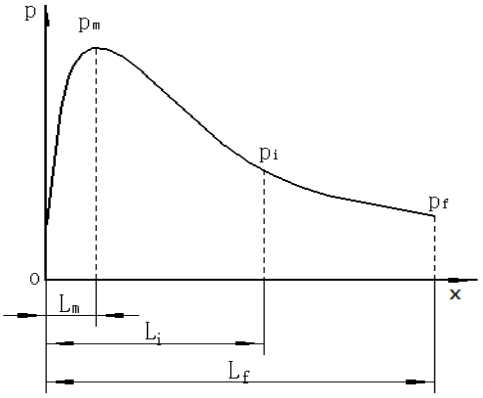

Figure 3. Bottom pressure and travel curve of projectile

The projectile is analyzed without considring other forces (Fig. 7). The force from the sabot acting on the projectile F_{12} is equal to its reaction force F_{21} in numerical value and opposite in direction. The projectile is embedded in the sabot then move together with the same speed after firing. The mass loss of projectile is set as φm_2 to represent various loss factors. Then Eq.(9) is obtained as follows:

$$\begin{aligned} &\varphi m_2\frac{dv}{dt} = F_{12} \\ &\varphi m_2\frac{dv}{dt}\frac{dx}{dx} = \varphi m_2 v\frac{dv}{dx} = p_{12}(x) = p_{21}(x) = kS_{dw}x, \quad x \le L_m \end{aligned} \tag{9}$$

When the projectile and sabot move L_m, Eq.(10) can be get as follows:

$$k = \frac{\varphi m_2}{S_{dw}}\left(\frac{v_m}{L_m}\right)^2 \tag{10}$$

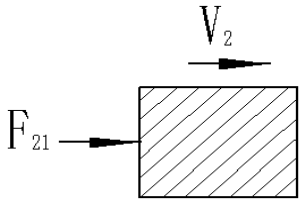

Figure 7. Force analysis of projectile

Taking Eq.(10) into Eq.8, Eq.(11) can be acquired as follows:

$$v_m^2 = \frac{2p_{cs}V_{cq}}{m_1\varphi(\gamma-1)}[1-\frac{V_{cq}^{\gamma-1}}{(V_{cq}+S_f L_m)^{\gamma-1}}]\cdot\frac{1}{1+\frac{m_2}{2m_1}} \tag{11}$$

According to Eq.(11), the relation curves between v_m and L_m, v_m and m_1 can be drawn as Fig. 8(a)~(b). Some conclusions can be deduced from the relation curves:

- There are direct proportion relation between v_m and L_m. If L_m increases, the maximum velocity v_m will increase.
- If the total mass of projectile and sabot is constant, the bigger m_1, the bigger v_m.

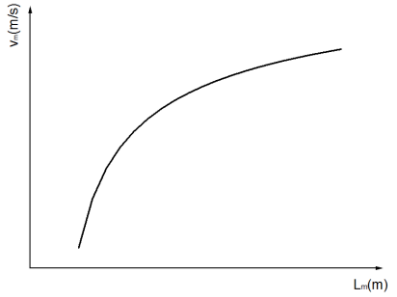

(a) The relation curve between v_m and L_m

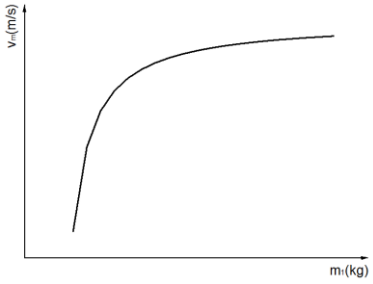

(b) The relation curve between v_m and m_1

Figure 8. The relation curves deduced from Eq.(11)

4. Experimental verification

From Fig.6, when projectile travels L_m and the velocity of it reaches v_m, the pressure exerted on it becomes the maximum. With the distance increasing, the pressure in launching tube decreases, but the projectile is still accelerated during the whole launching process. Its velocity v_e at the end position of gun barrel must be higher than v_m. The pressure calculated by v_e will be higher than the actual maximum pressure. Replacing v_m as v_e to analyze the strength of sabot will be more reliable.

The experimental device is shown in Fig. 9. The diameter of the metal projectile is 25mm, the air gun's tube diameter is 65mm, the sabot's length l is 100mm, the design impact speed v_e is 150m/s, the p_{cs} value is 0.132MPa after calculating by above equations. The calculation parameters of this high speed impact experiment are shown in Table 1.

Figure 9. Impact test device

Table 1. The parameters of high-speed impact experiments

Name	Value
$\mu_g\ (kg g mol^{-1})$	2.8e-2
γ	1.41
$V_{cq}\ (m^3)$	0.08482
$T\ (K)$	300
$R\ (J/(mol gK))$	8.31
K	1.1
$p_{cs}\ (Pa)$	0.29E6
$S_f\ (m^2)$	3.3e-3
$S_{dw}\ (m^2)$	4.9e-4
$m_1\ (kg)$	0.013
$m_2\ (kg)$	0.128
$v_m\ (m/s)$	150

According to Table 1, Eq.(3) and Eq.(11), the distance L_m can be calculated by the velocity at the end of launching tube. Then the pressure between projectile and sabot can be achieved based on Eq.(9) and Eq.(10). This pressure will be higher than the calculating result with v_m. The results are obtained as follows: $p_{12} = p_{21} = 2.68MPa, L_m = 3.05m$. In other words, when the sabot and the projectile as a whole run to the middle position of the launch tube, the pressure is expected to reach the maximum of 2.68MPa. Because the damage between projectile and sabot is obviously shear failure, the shear stress is calculated as follows:

$$\tau = \frac{p_{12} S_{dw}}{\pi d_{dw}(l - l_k)} \tag{12}$$

Where d_{dw} is the diameter of projectile， l is the length of sabot， l_k is the depth of hole in projectile.

If we put the related parameters of projectile and sabot ($d_{dw} = 0.025m, l = 0.1m, l_k = 0.03m$) into Eq. (12), we can get τ ($\tau = 0.24MPa$). The shear test is carried out, the compressive strength and shear strength of the sabot are 0.15MPa and 0.02MPa. They are less than 0.24MPa, which means that the damage will occur. This calculation result is consistent with the examination phenomenon(Fig. 3), the projectile penetrated through the sabot and formed a hole.

The material of sabot was changed to increase its density and shear strength. Three new sabots were made, Fig.10(a) and (b) were polyurethane foams,whose density were 200 kg/m^3 and 300 kg/m^3. Fig.10(c) was made by ethylene vinyl acetate (short for EVA) foam. Their shear strength were 0.12 MPa ,0.18 MPa and 0.4MPa respectively and higher than the calculation value. The three material were all used and the experiments were all successful. The density of EVA foam was only 40 kg/m^3, and it was the best choice for sabot among the three material.

(a) Polyurethane foam (b) Polyurethane foam (c)EVA foam

Figure 10. Sabot with big density

5. Conclusions

In view of the separation of projectile and sabot in high-speed impact experiment, the dynamics of high speed impact and the bearing strength of the sabot were analyzed and deduced. The model of the interaction between the sabot and the projectile is established, and the correctness of the model is verified. According to the relationship model, the following conclusions can be acquired:

- Under the same conditions, the lighter the sabot, the larger the maximum stress between sabot and projectile.
- Under the same conditions, the heavier the projectile, the larger the maximum stress between sabot and projectile.
- The higher the impact speed, the larger the maximum stress between sabot and projectile.

This model is acquired by theoretical derivation, but it still needs more data to verify its validity, and the difference between theoretical data and real data should be researched deeper.

6. Acknowledgments

This work is supported by the Major Project of High-end CNC Machine Tools and Basic Manufacturing Equipment of China (2014ZX04011021), Project of Shaanxi Province(2016KTCQ01) .

7. References

[1] Rob R, Sivaiah A Et Al, Sivaiah A, Nageshwar R V and Syed A H, Simulation studies on the effect of projectile nose shape impacting on aluminum plates, *Int J Mech Eng & Robto Res*,3(1),2014:119-122.
[2] Yan L, Experimental research on high impact test,*Taiyuan: North University of China*, 2008:p.7-8
[3] Xu H X, Study on the structure of elastic material of armor piercing projectile, *Nanjing: Nanjing University of Science and Technology*, 2007:p.3.
[4] Yang SH L, Plastic and composite material sabot, *Missile Tech*, 1998(2):p.42-45.
[5] Tang Z X, Lin G B, Sun S H and Lin W. Application of new material technology in sabot, *Ship Elec Eng*, 35(3), 2015: p.158-160.
[6] Celmins, I. Subscale simulation of sabot separation. Proceedings - *28th Int Symposium on Ballistics, BALLISTICS 2014, Atlanta, GA, United states*, 2014: p.860-869.
[7] Takeuchi, F and Matsuo A. Numerical investigation of sabot separation process in a ballistic range using moving overlapped grid method[C]. *Proceedings -51st AIAA Aerospace Sciences Meeting including the New Horizons Forum and Aerospace Exposition 2013, Grapevine, TX, United states*,2013:p.025003.
[8] Huang Z G, Wessam M E and Chen ZH. Numerical investigation of the three-dimensional dynamic process of sabot discard. *J Mech Sci & Tech,* 28 (7) , 2014: p.2637-2649.

[9] Minnicino, M A. Structural dynamics of despun kinetic energy projectiles launched with composite sabots. *Proceedings-27th International Symposium on Ballistics, BALLISTICS 2013. Freiburg, Germany,*2013:p.428-439.
[10] JH Choi. A Study on the Fabrication of the Composite Sabot for a Kinetic Energy Projectile, Brain Research,9(3) ,2006:p.15
[11] Acharya, R S and Naik S D, Motion analysis during sabot opening process. *Defence Sci J.* 57(2) , 2007:pp.229-241.
[12] Mikhail, A G and Heavey K R. Sabot opening lift force: Analysis, CFD, and test.*38th Aerospace Sciences Meeting and Exhibit.Reno, NV, United states*, 2000:p.1-9.
[13] Wang J G, Principle and technology of gas gun,*Beijing: National Defence Industry Press,* 2001: p.43.
[14] Jin Zh M, Yuan Y X and Song M. Modern interior ballistics,*Beijing: Beijing Institute of Technology press*, 1992